Wirelessly Operated, Implantable Optoelectronic Probes for Optogenetics in Freely Moving Animals

Yu Zhao, Changbo Liu, Zhixiang Liu, Wenhan Luo, Lizhu Li, Xue Cai, Dong Liang, Yuanzhe Su, He Ding, Qiang Wang, Lan Yin, Jisong Guan, Minmin Luo, and Xing Sheng

***Abstract*— Recording and interrogating brain activities using optical methods have become emerging technologies in neuroscience. Traditional tools for optogenetic stimulation in the deep brain are mostly based on implantable fibers, imposing constraints on the animal movement. Recently developed microscale light-emitting diodes (micro-LEDs), which can be wirelessly operated, serve as injectable light sources that directly interact with neural systems. Here, we exploit a wirelessly controlled, implantable system for optogenetic studies in behaving animals. Thin-film indium gallium nitride (InGaN)-based blue micro-LEDs transferred onto flexible probes are injected into the animal brain and optically activate channelrhodopsin-2 expressing neurons. A customized circuit module with a battery is employed to modulate the micro-LED, which is remotely controlled at a distance up to 50 m via 2.4-GHz radio frequency communications. The systems are implemented on freely moving mice, and demonstrate optogenetic modulation of locomotive behaviors in vivo. Moreover, independent and synchronous control of multiple animals is accomplished with the communication unit in the design circuit. The proposed system provides the potential for advanced optical neural interfaces and offers solutions to study complicated animal behaviors in neuroscience research.**

***Index Terms*— Implantable devices, micro-light-emitting diodes (LEDs), optogenetics, wireless operation.**

I. Introduction

EXPLORING advanced techniques to decode and modulate neural signals are critically important in understanding functions of the mammalian brain, which could further help to develop novel methods to treat neurological diseases and design next-generation neuromorphic computing systems [1], [2]. Along with the recent development of genetically encoded actuators and indicators, optical methods have been increasingly applied to monitor and control neural activities [3]. In particular, different types of microbial opsins can be employed as optogenetic tools to enable specific and precise neural signal activation or inhibition with light [4]. As advanced optical neural interfaces, various materials, devices, and systems are investigated to deliver light power and signals into the deep nervous tissue [5]. In neuroscience laboratories, commonly used tools for light delivery are based on optical fibers made of silica, which link the biological tissue with external optical components such as light-emitting diode (LED) or laser-based light sources, bandpass filters, and so on [6]. Such bulky, tethered systems constrain the free moving of animals, thus complicating the study of motion related behaviors. Untethered devices can potentially be realized by combining implantable fibers or waveguides with on-chip LED or laser sources [7]–[10]. However, low LED/fiber coupling efficiencies or high power consumptions of lasers make the system miniaturization impractical. Furthermore, the high mechanical stiffness of inorganic fibers and waveguides results in their unfavorable compatibility with biological tissues.

Recently developed thin-film, microscale optoelectronic devices provide promising solutions to realize ideal optical biointerface [11]. By exploiting novel fabrication strategies such as epitaxial liftoff and transfer printing, ultraminiaturized and high-performance optoelectronic devices such as LEDs and photodetectors based on single crystalline silicon and III–V compound semiconductors can be formed and integrated into flexible, stretchable, and even biodegradable

Manuscript received November 12, 2018; accepted November 15, 2018. Date of publication December 5, 2018; date of current version December 24, 2018. This work was supported in part by the National Natural Science Foundation of China under Grant 61874064 and in part by the Beijing Innovation Center for Future Chips. The review of this paper was arranged by Editor M. M. Hussain. *(Y. Zhao and C. Liu contributed equally to this work.) (Corresponding author: Xing Sheng.)*

Y. Zhao, C. Liu, L. Li, X. Cai, D. Liang, Y. Su, Q. Wang, and X. Sheng are with the Department of Electronic Engineering, Beijing National Research Center for Information Science and Technology, Tsinghua University, Beijing 100084, China (e-mail: xingsheng@tsinghua.edu.cn).

Z. Liu is with the National Institute of Biological Sciences, Beijing 102206, China.

W. Luo is with the Peking-Tsinghua Center for Life Sciences, Beijing 100871, China, also with the School of Life Sciences and Technology, ShanghaiTech University, Shanghai 201210, China, and also with the Academy for Advanced Interdisciplinary Studies, Peking University, Beijing 100871, China.

H. Ding is with the School of Optics and Photonics, Beijing Institute of Technology, Beijing 100081, China.

L. Yin is with the School of Materials Science and Engineering, Tsinghua University, Beijing 100084, China.

J. Guan is with the School of Life Sciences and Technology, ShanghaiTech University, Shanghai 201210, China.

M. Luo is with the National Institute of Biological Sciences, Beijing 102206, China, also with the School of Life Sciences, Tsinghua University, Beijing 100084, China, and also with the Chinese Institute for Brain Research, Beijing 102206, China.

Color versions of one or more of the figures in this paper are available online at http://ieeexplore.ieee.org.

Digital Object Identifier 10.1109/TED.2018.2882397

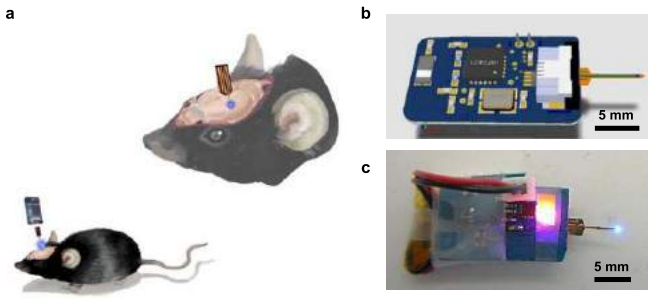

Fig. 1. (a) Cartoon diagram of the wireless, implantable system for *in vivo* optogenetics. (b) 3-D schematic illustration of the system. (c) Photograph of a prototype system powering a probe with a blue micro-LED.

platforms [12]–[15]. These devices can be directly injected into mammalian central and peripheral nervous systems, generating light signals and directly interacting with tissues. Compared to aforementioned silica fiber-based counterparts, such micrometer-scale devices exhibit superior performance in terms of their geometries, mechanical flexibility, and stretchability, as well as versatile functionalities. In addition, these microscale devices can be easily integrated with electronic control units that enable wireless power and signal transmission. Representative results include microscale LED (micro-LED)-based optogenetic probe powered by batteries, infrared light, radio frequency (RF) antennas, or inductive coils [16]–[19]. With these strategies, *in vivo* optogenetic modulation in behaving animals has been successfully accomplished. Nevertheless, few studies are able to demonstrate independent control of multiple animals due to the limitation of the power transfer techniques. Furthermore, output light stability and power transmission distances are limited when near-field coupling techniques are applied. Independent, remote control of multiple receivers is crucial for studying complicated locomotion and social behaviors in groups of animals. In this paper, we develop an implantable and wirelessly operated system for optogenetics, which integrates fully injectable micro-LEDs on flexible probes with a miniaturized control circuit. Thin-film, microscale indium gallium nitride (InGaN) blue LEDs serve as light sources to optically activate channelrhodopsin-2 (ChR2) expressing neurons. The LED output power is adjustable and stabilized with a removable circuit module powered with a rechargeable battery. Through 2.4-GHz RF communication, the injectable LEDs are remotely controlled. Implanted into the deep brain of free moving mice, the LED microprobes exhibit stable light output in chronic studies. *In vivo* optogenetic stimulations of the hippocampus (HPC) and cuneiform nucleus (CnF) demonstrate the system's utility for simultaneous behavioral interventions of multiple animals. Optogenetic experiments to various nucleus are possible by adjusting frequency, current, and other parameters of the micro-LED synchronously.

II. Design, Fabrication, and Characterization

The conceptual illustration of the wireless, implantable optogenetic microprobe system is displayed in Fig. 1. As shown in Fig. 1(a), a blue emitting micro-LED is integrated

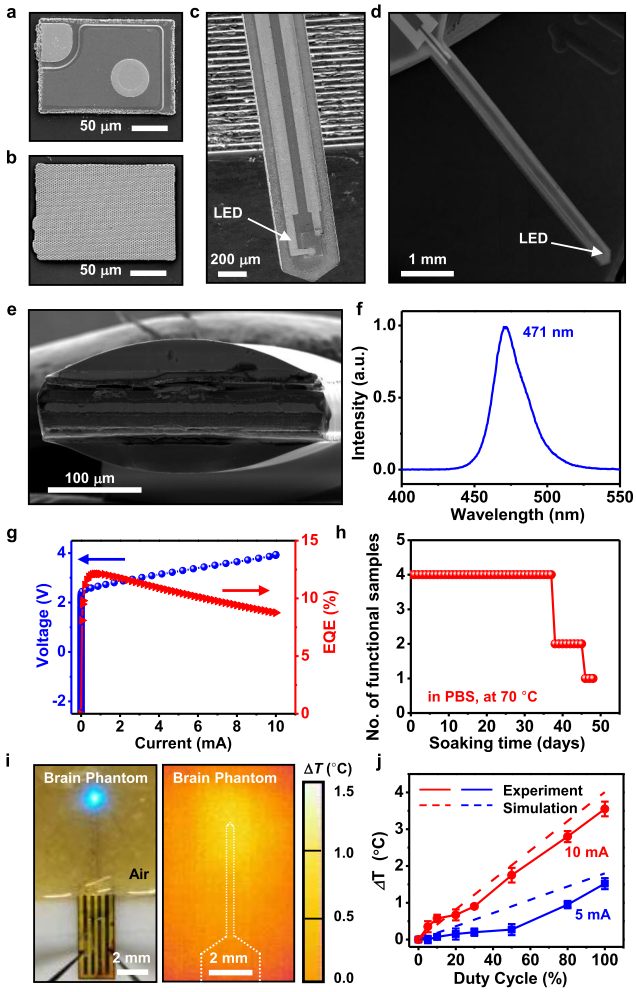

Fig. 2. (a) Front side and (b) back side SEM images of a thin-film InGaN micro-LED. (c) Front view and (d) side view SEM images of a microprobe with a printed and metallized micro-LED. (e) Cross-sectional view of the probe with encapsulation layers. (f) EL spectrum of the micro-LED with an emission peak at 471 nm. (g) Measured output voltage (blue curve) and external quantum efficiency (red curve) as a function of injection current for the InGaN micro-LED. (h) Number of functional micro-LEDs as a function of soaking time in PBS solutions at 70 °C. (i) Photograph of a micro-LED probe implanted into a brain phantom (left) and infrared thermograph (right) (injection current 10 mA, pulse frequency 20 Hz, duty cycle 20%). (j) Comparison of measured and simulated temperature rises of the brain phantom at LED injection currents of 5 and 10 mA with different duty cycles.

on a thin-film, flexible probe substrate that is implanted into the target nucleus expressing specific photoreceptors in living animals (for example, mice). Under nontesting conditions, only the LED microprobe is attached to the animal. When optogenetic stimulations are needed, a circuit module with all the control units (RF chips, antennas, and batteries) is connected to the LED probe through standard fixtures. Fig. 1(b) and (c) present the schematic and the photograph of the implantable system, respectively.

In the proposed system, the micro-LED is the key device that directly interacts with the animal neuronal system. Fig. 2 shows the structural, optoelectronic, thermal characteristics, and stability of the micro-LED. InGaN-based blue LEDs are epitaxially grown on patterned sapphire substrates and

lithographically formed. Release by the laser liftoff technique results in freestanding thin-film micro-LEDs, with lateral dimensions of 180 μm × 125 μm and a thickness of 7 μm. Fig. 2(a) and (b), respectively, shows the scanning electron microscope (SEM) images of front and back surfaces of an epitaxially released InGaN micro-LED. Using prepatterned polydimethylsiloxane (PDMS) stamps, the micro-LEDs are transferred onto flexible substrates made of double sided copper (Cu) electroplated polyimide (thickness: 18 μm Cu/25 μm polyimide/18 μm Cu, from DuPont). Compared with rigid probes based on silicon or glass, the use of polyimide mitigates mechanical mismatch with the soft brain tissue, thereby reducing the tissue inflammation response and improving the biocompatibility [20]. In addition, the metal-organic hybrid structures efficiently facilitate the heat dissipation during LED operations without affecting the probe's mechanical flexibility [12]. Subsequent process steps, which include photolithography, metal deposition, laser milling, and encapsulation, define the shape of the LED microprobe, with a width of about 300 μm, a thickness of about 140 μm, and a length of about 5 mm [Fig. 2(c) and (d)]. Sputtered layers of 10 nm Cr/800 nm Cu/200 nm Au serve as the metalized electrode, and dip-coated polyisobutylene (8% w/v in heptane, thickness ~7 μm, from J&K Scientific) and PDMS (mixed at 10:1 ratio, thickness ~30 μm, Sylgard 184, DowCorning) layers [21] work as a waterproof encapsulation. Both layers are cured at 70 °C for 1 h. The cross-sectional view SEM image in Fig. 2(e) illustrates that the entire probe is protected by the encapsulation layers with thicknesses of ~40 μm on both sides. It is noted that this probe geometry is smaller compared to conventional silica fibers, which typically have a diameter of 220 μm [6]. Before system integration, the electrical, optical, and thermal properties of the LED microprobe are measured with results summarized in Fig. 2(f)–2(j). The electroluminescence (EL) spectrum of the blue micro-LED [Fig. 2(f)] presents a peak wavelength of 471 nm, which matches to the absorption spectrum of the light-gated cation channel ChR2 [22]. As shown in Fig. 2(g), the current and voltage characteristics indicate that the micro-LED has a turn-on voltage of about 2.5 V and its injection current reaches about 10 mA at about 4 V. Its maximum external quantum efficiency is measured to be about 12%. To evaluate the stability of micro-LED probes in the physiological environment, four encapsulated probes are immersed in phosphate-buffered saline (PBS) solution at 70 °C. As shown in Fig. 2(h), all the probes exhibit stable operation for up to 35 days. We expect that the micro-LEDs can work for a longer time (several months) without performance degradation in the physiological environment (at ~37 °C) *in vivo*. The thermal property is also an indispensable parameter associated with all the implantable microprobes. To avoid irreversible tissue damages, the temperature rise for probes operated in mammal brains should be limited to a safe range (typically within about 1 °C). By inserting the operating LED probes into the hydrogel-based brain phantom (thickness ~0.5 mm) at a depth of about 6.3 mm, their thermal effects are evaluated with an infrared camera (FOTRIC 228) [Fig. 2(i)]. The brain phantom is made of agarose (0.5% w/v), hemoglobin (0.2% w/v), intralipid (1% w/v), and phosphate buffer

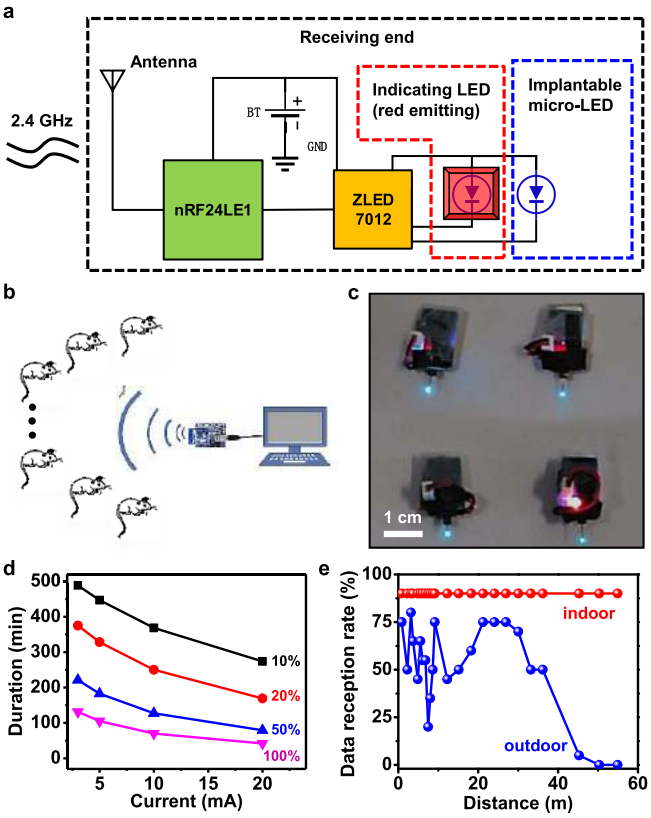

Fig. 3. (a) Block diagram showing the operational principle for the circuit system. (b) Schematic of the system working at a multireceiver mode. (c) Photograph showing multiple receivers with micro-LED probes independently controlled by remote systems (see videos in supporting information). (d) Operational durations of the system powered by a rechargeable battery (capacity: 35 mAh) as a function of LED output current with varied duty cycles. (e) Transmission reliability measured as a function of communication distance in indoor and outdoor environments.

solutions (98.3% w/v). After stirring, the mixed liquid is heated to boiling and then naturally cooled to room temperature. Maximum temperature rises on the phantom surface are measured at various injection currents and pulse duty cycles. Results are plotted in Fig. 2(j) and consistent with finite-element analysis-based simulations. It can be seen that the tissue temperature rise can be mitigated to be below 1 °C above room temperature when the LED injection current is less than 10 mA and the duty cycle is less than 40%. At an injection current of 5 mA, the LED has an optical power density of ~82 mW/mm^2, which is much higher than the minimum light power needed to stimulate neurons (typically 1–10 mW/mm^2 [17]). As shown in following sections, these operation parameters are appropriate for *in vivo* optogenetic stimulation with minimum adverse effects related to heating.

The micro-LED on the flexible probe are connected and controlled by a customized circuit module with the design illustrated in Fig. 3(a). On the designed printing circuit board, a 2.4-GHz RF antenna accompanied with its matching circuit wirelessly receives command signals (LED ON and OFF time, current level, pulse frequency, duty cycle, target channels, and so on) from the sending end connected to a laptop computer. A microcontroller unit (MCU) (Nordic nRF24LE1 chip)

processes the signals to modulate the LED, with a maximum air data rate up to 2 Mbps. Between the MCU and the micro-LED, a chip (ZLED7012) converts the modulation signals to constant currents at 14 different levels from 1.8 to 20 mA, in order to stabilize the LED light output. A synchronously operated red-lighting LED (made by a blue LED covered with red phosphors [12]) is mounted on the printed circuit board (PCB) as an indicator for communication assessment. A distinctive feature of the module is related to its capability of independently controlling multiple receiving ends [Fig. 3(b)]. Different addresses can be assigned to multiple receivers can be assigned via programing the MCU. When the commands from the ex-transmitter matches with the address number of the receiving end, communication is built. Up to 1000 channels can be defined with three decimal digits. For demonstration, Fig. 3(c) presents that four different micro-LED probes can be independently operated with the designed module wirelessly controlled by the same sending end. The circuit is powered by a rechargeable lithium ion battery (with a capacity of 35 mAh). Compared to wireless energy transfer techniques based on RF [17], [18] or infrared irradiations [14], [19], rechargeable batteries provide a more stable energy supply and offer more freedom to the movement of animals. The entire PCB has a weight of 1.9 g (including the battery weight about 1.2 g) and a size of 10 mm $\times$ 18 mm. The system's size and weight can be further reduced by designing customized application-specified-integrated circuits and employing flexible PCBs. Fig. 3(d) illustrates the battery's operation time measured as a function of the LED injection at various duty cycles. Under a typical experimental condition for optogenetic studies (current $=$ 10 mA, duty cycle $=$ 20%), the battery lifetime can reach more than 4 h, which is adequate for most *in vivo* experiments. On the PCB, the antenna chip receives signals with constant gains at nearly all arrival angles. Fig. 3(e) presents its effective operation distances in indoor and outdoor environments. During the indoor test, the module's maximum communication distance reaches up to 55 m with a success rate $\geq$ 90%. Data reception rates decrease in outdoor tests, which is associated with interferences with electromagnetic noises in the environment. The transmission stability can be further improved by optimizing the circuit in the future.

III. Results and Discussion

Besides independent control of multiple objects, a notable advantage of our designed system over conventional fiber optics is the minimal interference among behaving animals. Throughout *in vivo* experiments, the animal care was in accordance with the institutional guidelines of Tsinghua University and National Institute of Biological Sciences in Beijing. Protocols were proved by Institutional Animal Care and Use Committee. As shown in Fig. 4(a), the mouse implanted with a micro-LED probe exhibit normal behaviors. During stimulation tests, the miniaturized control PCB can be mounted via standard fixtures, without affecting the animals' locomotive activities [Fig. 4(b)]. The traces of multiple mice with and without implanted systems are recorded and presented in Fig. 4(c) and (d), respectively. Although movements of mice

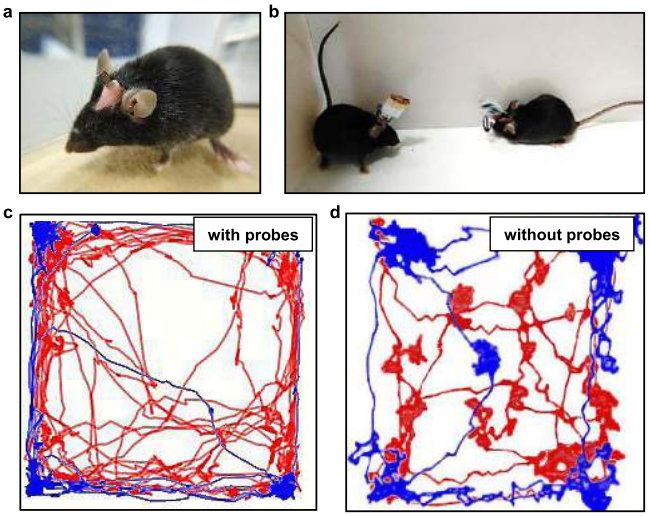

Fig. 4. *In vivo* evaluation of implantable systems on freely behaving mice. (a) Mouse with a micro-LED probe implanted subcranially. (b) Two mice mounted with wireless controlled systems including batteries in a test arena. (c) and (d) Recorded traces of activities for two mice (c) with and (d) without implanted systems in the test arena for 2 min (arena size: 50 cm $\times$ 50 cm).

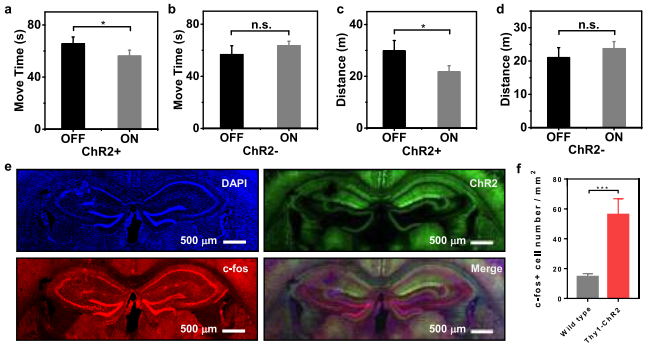

Fig. 5. *In vivo* optogenetic stimulation with wirelessly controlled micro-LED probes implanted into the HPC (control group $n = 4$, test group $n = 4$). Recorded moving time for mice (a) with and (b) without expressing ChR2 under the light on and off conditions. Recorded moving distance for mice (a) with and (b) without expressing ChR2 under light on and off conditions. For (a) and (c) $^{*}P < 0.05$, t test. (e) Immunostaining results of brain slices at the HPC expressing DAPI (blue), ChR2 (green), and c-fos (red), as well as the merged image. (f) Comparison of c-fos expressing cell population between wild type and Thy1-ChR2 mice ($^{***}P < 0.001$, t-test). DAPI, 4', 6-diamidino-2-phenylindole; ChR2, Channelrhodopsin-2; c-fos, Finkel-Biskis-Jinkins osteosarcoma oncogene.

are not exactly the same, the uniform trace distribution reveals little interference between the mice in the arena. Therefore, the wirelessly operated devices impose negligible effects on animals' sociological behaviors.

For proof-of-concept demonstration, *in vivo* behavioral studies are performed by applying our designed systems in different brain regions of freely moving mice, as shown in Figs. 5 and 6. First, we choose the HPC (anteroposterior (AP): -2.0 mm, mediolateral (ML): -1.5 mm, dorsoventral (DV): -1.5 mm, nucleus size of $\sim$2.27 mm^3) as the study region (Fig. 5), in which optogenetic activation could induce seizure related abnormal locomotions [23]. In this experiment,

TABLE I
COMPARISON OF OPERATIONAL CHARACTERISTICS AMONG DIFFERENT WIRELESS CONTROL SYSTEMS BASED ON IMPLANTABLE MICRO-LEDS AND FIBERS USED IN OPTOGENETICS

	this work	ref. [8]	ref. [16]	ref. [17] [28]	ref. [18]	ref. [27]
LED size (μm³)	180 * 125 * 7	800 * 1600 * 1600	320 * 240 * 140	50 * 50 * 7	320 * 240 * 140	270 * 220 * 50
Cross-sectional area of the probe (μm²)	300 * 140	$\Phi = 200$ [a]	700 * 100	400*270 [b]	$\Phi = 350$	350 * 130
Communication distance (m)	55	1	4	1	< 0.1	0.3
weight (g)	1.9	1.6	2.9	2.0	0.05	0.03
Independent control of multiple receivers	Yes	Yes	Yes	No	No	No
types of communication	2.4 GHz RF	2.4 GHz RF	2.4 GHz RF	910 MHz RF	1.5 GHz RF resonant cavity	13.56 MHz inductive coupling
Energy harvesting	battery	battery	battery	antenna	antenna	antenna

[a] The probe is a silica fiber with externally coupled LEDs.
[b] The probe thickness (270 μm) includes a thin-film needle (20 μm thick) for permanent implantation and a hard needle (250 μm thick) for temporary injection, which is retrieved after implanting.

Thy1-ChR2 mice are chosen since they express ChR2 in HPC excitatory neurons. Micro-LED probes are implanted into the HPC of Thy1-ChR2 mice at a depth of 1.5 mm targeting to the CA1 subregion. Optogenetic stimulations are conducted after recovery for 1 week. The behaviors of the mice are recorded in an 8-min stimulating period, which comprises a 2-min adaptive interval, a 2-min light pulse (LED current 5 mA, power density about 82 mW/mm^2, pulse frequency 20 Hz, duty cycle 20%), a 2-min resting, a 2-min light pulse (5 mA, 82 mW/mm^2, 20 Hz, 20%) and a 2-min resting, successively. Both the treated and control groups include four mice and are tested under the same conditions. We change the current according to the mice behavior and the power density of LEDs in [16]–[18]. The moving time and the traveling distance of the tested mice are statistically analyzed and compared in Fig. 5(a)–5(d). For ChR2 expressing mice (ChR2+), measured move times and distances in light-on periods are lower than light-off periods by 14% and 27%, respectively (t-test, significant difference $^*P < 0.05$). By contrast, behaviors in the control group (wild type, ChR2-) exhibit no significant difference between light-on and light-off periods. These results indicate that optogenetic stimulations mildly inhibit locomotion in ChR2 expressing mice. After behavior studies with light treatment, mice are perfused for immunostaining tests. Fig. 5(e) illustrates the fluorescence images of brain slides expressing DAPI (4', 6-diamidino-2-phenylindole), ChR2, c-fos (a marker for activated neuron), and merged image. Averaged c-fos labeled cell amounts are plotted and compared in Fig. 5(f), which shows that light treatment induces a much higher amount of c-fos expressing cells in ChR2 expressing mice than in the control group (significant difference $^{***}P < 0.001$).

We further explore the use of our implantable probe in the CnF (AP: −4.9 mm, ML: +0.95 mm, DV: −3.0 mm, nucleus size of ∼0.17 mm^3) as shown schematically in Fig. 6(a). When the blue light is turned on, optical stimulations lead to obvious locomotion changes, in agreement with previous reports [24], [25]. The control of multiple channels is demonstrated by placing two mice (C57 BL/6N) in the same test arena, as shown in Fig. 6(b). By sending different commands to two corresponding receiving ends, we are able to independently modulate the animals' behaviors and study their social interactions. Additional statistical analyses are presented in Fig. 6(c). Similar to the experimental procedures mentioned in Fig. 5, optogenetic stimulations are performed after the recovery from the expression of ChR2 and the injection of micro-LED probes. Each testing period contains three equally sequential steps including before, during, and after light stimulation (3, 5, or 10 s). The speeds of movement at different steps are extracted from captured videos using a standard optical flow based method in MATLAB [26]. We confirm that light stimulation in the CnF significantly enhances locomotive actions. The results are 22, 31, and 15 (all in arbitrary units) in before, during and after steps, respectively. Under light stimulation, mice expressing ChR2 move at a much higher speed compared to mice without ChR2. Fig. 6(d) illustrates the immunostaining results (DAPI, ChR2, c-fos, and merged) of brain sections after light stimulation and perfusion.

The implantable micro-LED based optoelectronic probe presented here holds the capability for a long lifetime, wireless, and remote optogenetic interrogation in multiple objects. With these features, the system clearly demonstrates its advantages over conventional fiber optic-based techniques. In recent

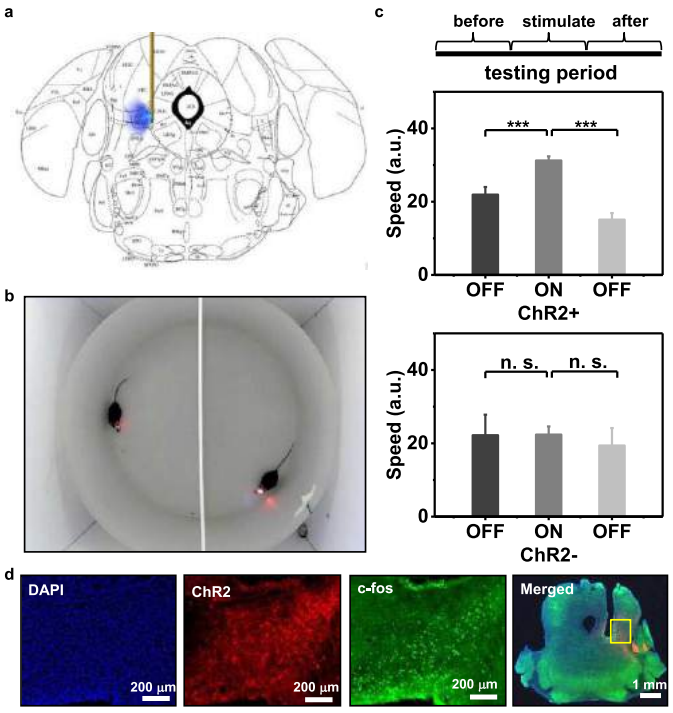

Fig. 6. *In vivo* optogenetic stimulation with wirelessly controlled micro-LED probes implanted into the CnF. (a) Schematic of the stimulated region with a micro-LED probe in the mouse brain. (b) Independent control of two mice within a test arena. See videos provided in supporting information. (c) Recorded moving speed comparing mice with (up) and without (bottom) expressing ChR2 at light on and off states. The time periods for "before", "stimulating", and "after" are 3s, 5s or 10s, equally (control group $n = 3$, test group $n = 3$, $^{***}P < 0.001$, t test). (d) Immunostaining results of brain slices near the implanted region expressing DAPI (blue), ChR2 (red), and c-fos (green), as well as the merged image.

years, several wireless operated tools based on implantable optoelectronic devices have been developed and demonstrated *in vivo* optogenetic stimulation in freely moving animals. We compare our wireless optogenetic probe with some representative works in literature [8], [16]–[18], [27], [28] and some key parameters are summarized in Table I. Among all these systems, its major advantages include: 1) it holds a small size by using epitaxially released micro-LEDs on flexible substrates, which minimizes the lesion area associated with the invasive injection; 2) the battery-powered circuit offers more freedom to animals than energy harvesters based on near-field electromagnetic wave coupling; 3) the implementation of the MCU and the RF antenna in the circuit module allows long-distance communication (up to about 50 m), which is far superior to other systems; and 4) it enables independent control of multiple receiving objects, which creates vast opportunities in studying complex neurological behaviors in a group of animals, as demonstrated in Figs. 3 and 6.

IV. Conclusion

The heterogeneous integration of thin-film, microscale optoelectronic devices on flexible probes offers an extendable platform for versatile functionalities. Examples for future endeavors include the placement of multiple micro-LEDs at different locations for multisite optogenetic stimulations, or stacking LEDs of different colors for simultaneous activation/inhibition in a single nucleus. Besides optogenetic stimulations, micro-LEDs, photodetectors [13], electrodes [29], [30], and microfluidic channels [31] could be combined to realize multimodal electrical-optical-chemical, close-loop monitor, and control of neural activities. Without constraints imposed by tethered fibers, it is also envisioned that similar systems would be applicable for neuroscience studies in large animals including nonhuman primates [32]. In addition, implantable micro-LEDs with wireless power and signal transfer also show potential for clinical uses, including photodynamic therapies and tissue regeneration [33], [34]. In summary, results presented here offer viable routes to implantable optoelectronic devices for neuroscience studies and biomedical applications in general.

References

[1] T. R. Insel, S. C. Landis, and F. S. Collins, "The NIH BRAIN initiative," *Science*, vol. 340, no. 6133, pp. 687–688, May 2013, doi: 10.1126/science.1239276.
[2] M.-M. Poo, J.-L. Du, N. Y. Ip, Z.-Q. Xiong, B. Xu, and T. Tan, "China brain project: Basic neuroscience, brain diseases, and brain-inspired computing," *Neuron*, vol. 92, no. 3, pp. 591–596, Nov. 2016, doi: 10.1016/j.neuron.2016.10.050.
[3] M. R. Warden, J. A. Cardin, and K. Deisseroth, "Optical neural interfaces," *Annu. Rev. Biomed. Eng.*, vol. 16, no. 1, pp. 103–129, Jul. 2014, doi: 10.1146/annurev-bioeng-071813-104733.
[4] K. Deisseroth, "Optogenetics: 10 years of microbial opsins in neuroscience," *Nature Neurosci.*, vol. 18, no. 9, pp. 1213–1225, Aug. 2015, doi: 10.1038/nn.4091.
[5] R. Pashaie *et al.*, "Optogenetic brain interfaces," *IEEE Rev. Biomed. Eng.*, vol. 7, pp. 3–30, May 2014, doi: 10.1109/RBME.2013.2294796.
[6] L. A. Gunaydin *et al.*, "Natural neural projection dynamics underlying social behavior," *Cell*, vol. 157, no. 7, pp. 1535–1551, Jun. 2014, doi: 10.1016/j.cell.2014.05.017.
[7] G. Gagnon-Turcotte *et al.*, "A wireless optogenetic headstage with multichannel electrophysiological recording capability," *Sensors*, vol. 15, no. 9, pp. 22776–22797, Aug. 2015, doi: 10.3390/s150922776.
[8] S. T. Lee, P. A. Williams, C. E. Braine, D.-T. Lin, S. W. M. John, and P. P. Irazoqui, "A miniature, fiber-coupled, wireless, deep-brain optogenetic stimulator," *IEEE Trans. Neural Syst. Rehabil. Eng.*, vol. 23, no. 4, pp. 655–664, Jul. 2015, doi: 10.1109/TNSRE.2015.2391282.
[9] X. Bi, B. Fan, and W. Li, "Micro-lens-coupled LED neural stimulator for optogenetics," in *Proc. IEEE Biomed. Circuits Syst. Conf. (BioCAS)*, Oct. 2015, pp. 1–4.
[10] K. Kampasi *et al.*, "Dual color optogenetic control of neural populations using low-noise, multishank optoelectrodes," *Microsyst. Nanoeng.*, vol. 4, no. 1, p. 10, Jun. 2018, doi: 10.1038/s41378-018-0009-2.
[11] H. Xu, L. Yin, C. Liu, X. Sheng, and N. Zhao, "Recent advances in biointegrated optoelectronic devices," *Adv. Mater.*, vol. 30, no. 33, p. 1800156, Aug. 2018, doi: 10.1002/adma.201800156.
[12] L. Li *et al.*, "Heterogeneous integration of microscale GaN light-emitting diodes and their electrical, optical, and thermal characteristics on flexible substrates," *Adv. Mater. Technol.*, vol. 3, no. 1, p. 1700239, Jan. 2018, doi: 10.1002/admt.201700239.
[13] L. Lu *et al.*, "Wireless optoelectronic photometers for monitoring neuronal dynamics in the deep brain," *Proc. Nat. Acad. Sci. USA*, vol. 115, no. 7, pp. E1374–E1383, Feb. 2018, doi: 10.1073/pnas.1718721115.
[14] L. Lu *et al.*, "Biodegradable monocrystalline silicon photovoltaic microcells as power supplies for transient biomedical implants," *Adv. Energy Mater.*, vol. 8, no. 16, p. 1703035, Jun. 2018, doi: 10.1002/aenm.201703035.
[15] X. Sheng *et al.*, "Silicon-based visible-blind ultraviolet detection and imaging using down-shifting luminophores," *Adv. Opt. Mater.*, vol. 2, no. 4, pp. 314–319, Apr. 2014, doi: 10.1002/adom.201300475.
[16] M. A. Rossi, V. Go, T. Murphy, Q. Fu, J. Morizio, and H. H. Yin, "A wirelessly controlled implantable LED system for deep brain optogenetic stimulation," *Frontiers Integrative Neurosci.*, vol. 9, p. 8, Feb. 2015.
[17] T.-i. Kim *et al.*, "Injectable, cellular-scale optoelectronics with applications for wireless optogenetics," *Science*, vol. 340, no. 6129, pp. 211–216, Apr. 2013, doi: 10.1126/science.1232437.

[18] K. L. Montgomery *et al.*, "Wirelessly powered, fully internal optogenetics for brain, spinal and peripheral circuits in mice," *Nature Methods*, vol. 12, no. 10, pp. 969–974, Oct. 2015, doi: 10.1038/nmeth.3536.

[19] H. Ding *et al.*, "Microscale optoelectronic infrared-to-visible upconversion devices and their use as injectable light sources," *Proc. Nat. Acad. Sci. USA*, vol. 115, no. 26, pp. 6632–6637, Jun. 2018, doi: 10.1073/pnas.1802064115.

[20] H. C. Lee *et al.*, "Histological evaluation of flexible neural implants; flexibility limit for reducing the tissue response?" *J. Neural Eng.*, vol. 14, no. 3, p. 036026, May 2017, doi: 10.1088/1741-2552/aa68f0.

[21] V. K. Samineni *et al.*, "Fully implantable, battery-free wireless optoelectronic devices for spinal optogenetics," *Pain*, vol. 158, no. 11, pp. 2108–2116, Nov. 2017, doi: 10.1097/j.pain.0000000000000968.

[22] G. Nagel *et al.*, "Channelrhodopsin-2, a directly light-gated cation-selective membrane channel," *Proc. Nat. Acad. Sci. USA*, vol. 100, no. 24, pp. 13940–13945, Nov. 2003, doi: 10.1073/pnas.1936192100.

[23] G. M. Alexander *et al.*, "Remote control of neuronal activity in transgenic mice expressing evolved G protein-coupled receptors," *Neuron*, vol. 63, no. 1, pp. 27–39, Jul. 2009, doi: 10.1016/j.neuron.2009.06.014.

[24] L. F. Allen, W. L. Inglis, and P. Winn, "Is the cuneiform nucleus a critical component of the mesencephalic locomotor region? An examination of the effects of excitotoxic lesions of the cuneiform nucleus on spontaneous and nucleus accumbens induced locomotion," *Brain Res. Bull.*, vol. 41, no. 4, pp. 201–210, Jan. 1996, doi: 10.1016/S0361-9230(96)00165-7.

[25] M. Alam, K. Schwabe, and J. K. Krauss, "Reply: The cuneiform nucleus may be involved in the regulation of skeletal muscle tone by motor pathway: A virally mediated trans-synaptic tracing study in surgically sympathectomized mice," *Brain*, vol. 136, no. 10, p. e252, Oct. 2013, doi: 10.1093/brain/awt125.

[26] D. Fleet and Y. Weiss, *Optical Flow Estimation*. Boston, MA, USA: Springer, 2006, pp. 237–257.

[27] G. Shin *et al.*, "Flexible near-field wireless optoelectronics as subdermal implants for broad applications in optogenetics," *Neuron*, vol. 93, no. 3, pp. 509–521, Feb. 2017, doi: 10.1016/j.neuron.2016.12.031.

[28] J. G. Mccall *et al.*, "Fabrication and application of flexible, multimodal light-emitting devices for wireless optogenetics," *Nature Protocols*, vol. 8, no. 12, pp. 2413–2428, Dec. 2013, doi: 10.1038/nprot.2013.158.

[29] B. Ji *et al.*, "Flexible optoelectric neural interface integrated wire-bonding μ LEDs and microelectrocorticography for optogenetics," *IEEE Trans. Electron Devices*, vol. 64, no. 5, pp. 2008–2015, May 2017, doi: 10.1109/TED.2016.2645860.

[30] B. Fan, K.-Y. Kwon, R. Rechenberg, M. F. Becker, A. J. Weber, and W. Li, "A hybrid neural interface optrode with a polycrystalline diamond heat spreader for optogenetics," *Technology*, vol. 4, no. 1, pp. 15–22, Mar. 2016, doi: 10.1142/S2339547816400021.

[31] J.-W. Jeong *et al.*, "Wireless optofluidic systems for programmable *in vivo* pharmacology and optogenetics," *Cell*, vol. 162, no. 3, pp. 662–674, Jul. 2015, doi: 10.1016/j.cell.2015.06.058.

[32] A. Galvan *et al.*, "Nonhuman primate optogenetics: Recent advances and future directions," *J. Neurosci.*, vol. 37, no. 45, pp. 10894–10903, Nov. 2017, doi: 10.1523/JNEUROSCI.1839-17.

[33] A. Bansal, F. Yang, T. Xi, Y. Zhang, and J. S. Ho, "*In vivo* wireless photonic photodynamic therapy," *Proc. Nat. Acad. Sci. USA*, vol. 115, no. 7, pp. 1469–1474, Feb. 2018, doi: 10.1073/pnas.1717552115.

[34] K. Yamagishi *et al.*, "Tissue-adhesive wirelessly powered optoelectronic device for metronomic photodynamic cancer therapy," *Nat. Biomed. Eng.*, vol. 2, no. 7, pp. 1–10, Jul. 2018, doi: 10.1038/s41551-018-0261-7.

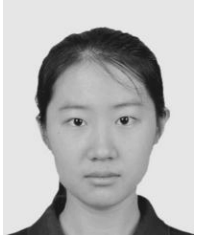

Yu Zhao received the B.Eng. degree from Chongqing University, Chongqing, China, in 2016. She is currently pursuing the Ph.D. degree with the Department of Electronic Engineering, Tsinghua University, Beijing, China.

Changbo Liu received the B.Eng. degree from Lanzhou University, Lanzhou, China, in 2008, and the Ph.D. degree from the Institute of Semiconductors, Chinese Academy of Sciences, Beijing, China, in 2013.

He is currently a Post-Doctoral Researcher with the Department of Electronic Engineering, Tsinghua University, Beijing.

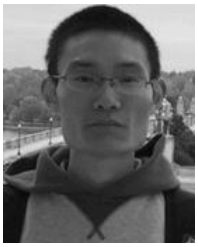

Zhixiang Liu received the B.S. degree in biology from Sichuan University, Chengdu, China, in 2009, and the Ph.D. degree from the National Institute of Biological Sciences, Beijing, China, in 2014.

He is currently a Post-Doctoral Fellow with the National Institute of Biological Sciences.

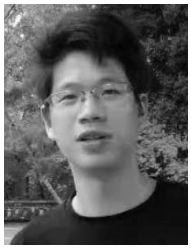

Wenhan Luo received the B.S. degree from the Department of Life Science, Peking University, Beijing, China, in 2013, where he is currently pursuing the Ph.D. degree with the Peking-Tsinghua Center for Life Sciences.

Lizhu Li received the B.Eng. degree from the University of Electronic Science and Technology of China, Chengdu, China, in 2016. She is currently pursuing the Ph.D. degree with the Department of Electronic Engineering, Tsinghua University, Beijing, China.

Xue Cai received the B.Eng. degree from the School of Optics and Electronics, Beijing Institute of Technology, Beijing, China, in 2018. She is currently pursuing the Ph.D. degree with the Department of Electronic Engineering, Tsinghua University, Beijing.

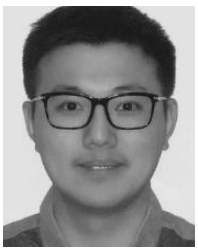

Dong Liang received the B.Eng. degree in electronic engineering from Tsinghua University, Beijing, China, in 2016, and the M.S. degree from the California Institute of Technology, Pasadena, CA, USA, in 2017.

He is currently a Software Engineer at Rubrik, Inc., Palo Alto, CA, USA.

Yuanzhe Su is currently pursuing the bachelor's degree with the Department of Physics, Tsinghua University, Beijing, China.

He Ding received the Ph.D. degree from Ecole Centrale de Lyon, Écully, France, in 2016, and the Ph.D. degree from Tsinghua University, Beijing, China, from 2016 to 2018.

He is currently an Assistant Professor with the School of Optics and Photonics, Beijing Institute of Technology, Beijing.

Qiang Wang received the B.Eng. degree from the Changchun Institute of Optics and Fine Mechanics, Changchun, China, in 1999.

He is currently an Optical Engineer with the Department of Electronic Engineering, Tsinghua University, Beijing, China.

Lan Yin received the bachelor's degree from Tsinghua University, Beijing, China, and the Ph.D. degree from Carnegie Mellon University, Pittsburgh, PA, USA.

She is currently an Associate Professor with the School of Materials Science and Engineering, Tsinghua University.

Jisong Guan received the Ph.D. degree from the Institute of Neuroscience, Chinese Academy of Sciences, Beijing, China, in 2006.

He then received the post-doctoral training at the Massachusetts Institute of Technology, Cambridge, MA, USA. He is currently an Associate Professor with the School of Life Science and Technology, Shanghai Tech University, Shanghai, China.

Minmin Luo is currently a Professor with the School of Life Sciences, Tsinghua University, Beijing, China, and the Principle Investigator of the National Institute of Biological Sciences, Beijing. He is also serving as the Co-Director of the Chinese Institute for Brain Research, Beijing.

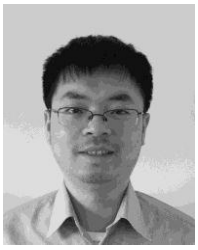

Xing Sheng received the B.Eng. degree from Tsinghua University, Beijing, China, in 2007, and the Ph.D. degree from the Massachusetts Institute of Technology, Cambridge, MA, USA, in 2012.

He is currently an Associate Professor with the Department of Electronic Engineering, Tsinghua University.

Figure S1

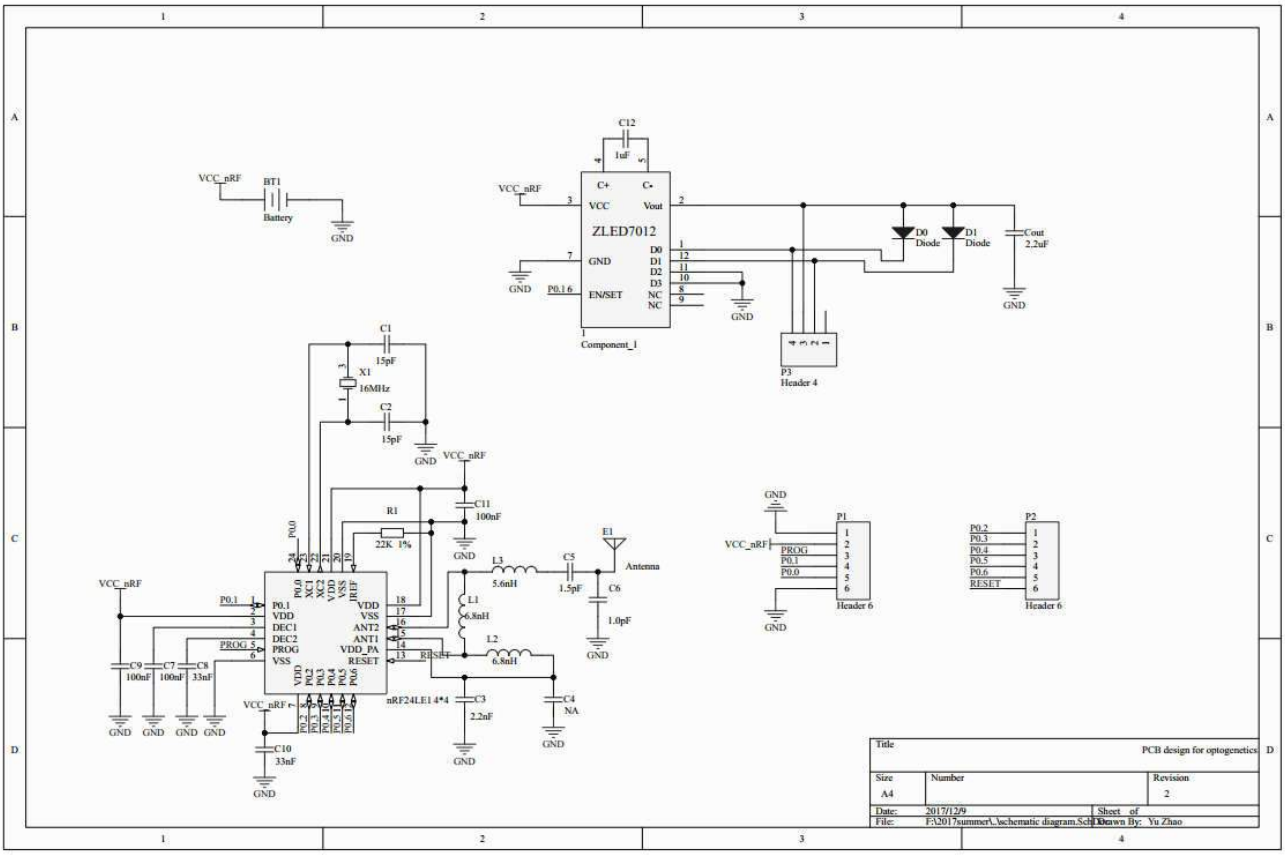

Figure S1. Schematic diagram of the wireless control circuit for the micro-LED probe.

Figure S2

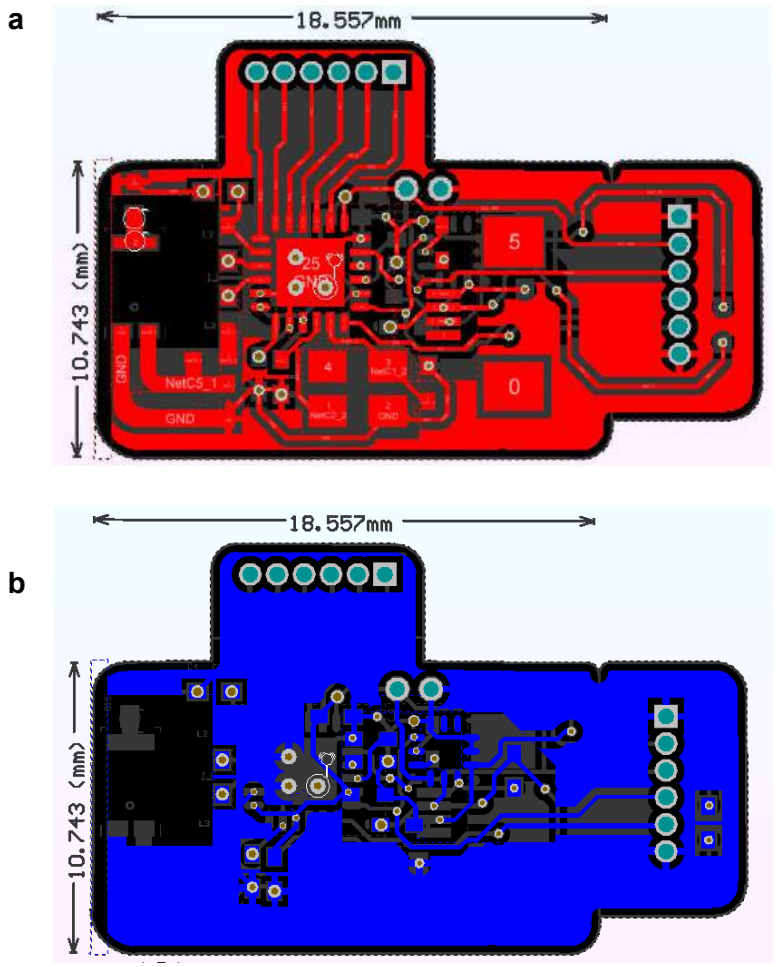

Figure S2. Layout of the designed printed circuit board. a) front view and b) back view.

Figure S3

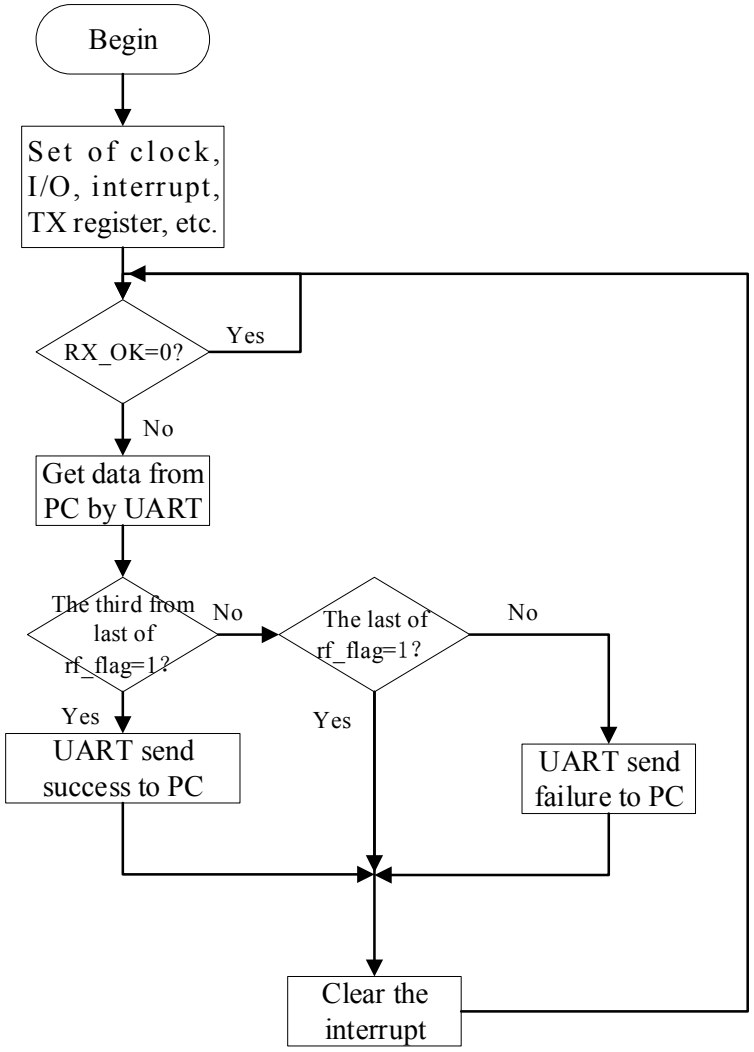

Figure S3. Flow diagram of the sending end program.

Figure S4

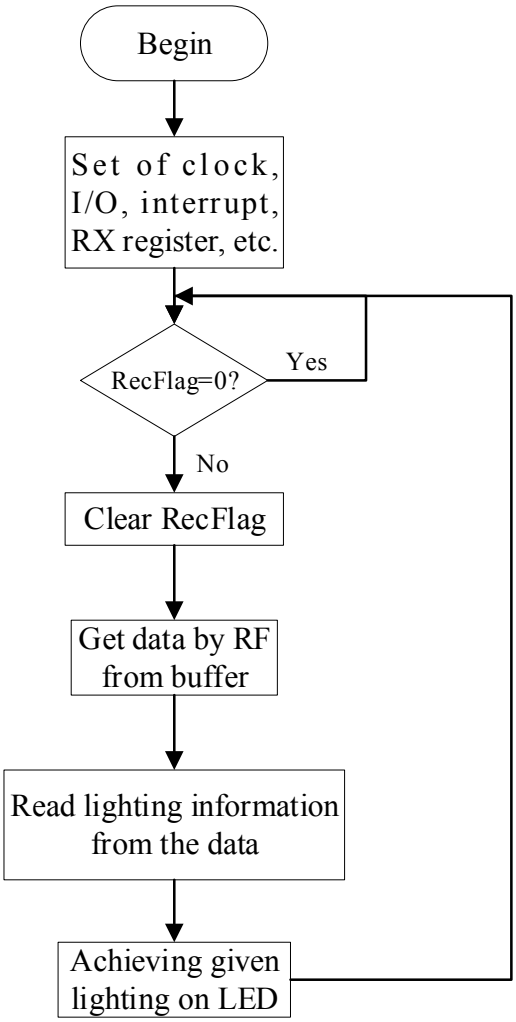

Figure S4. Flow diagram of the receiving end program.

Figure S5

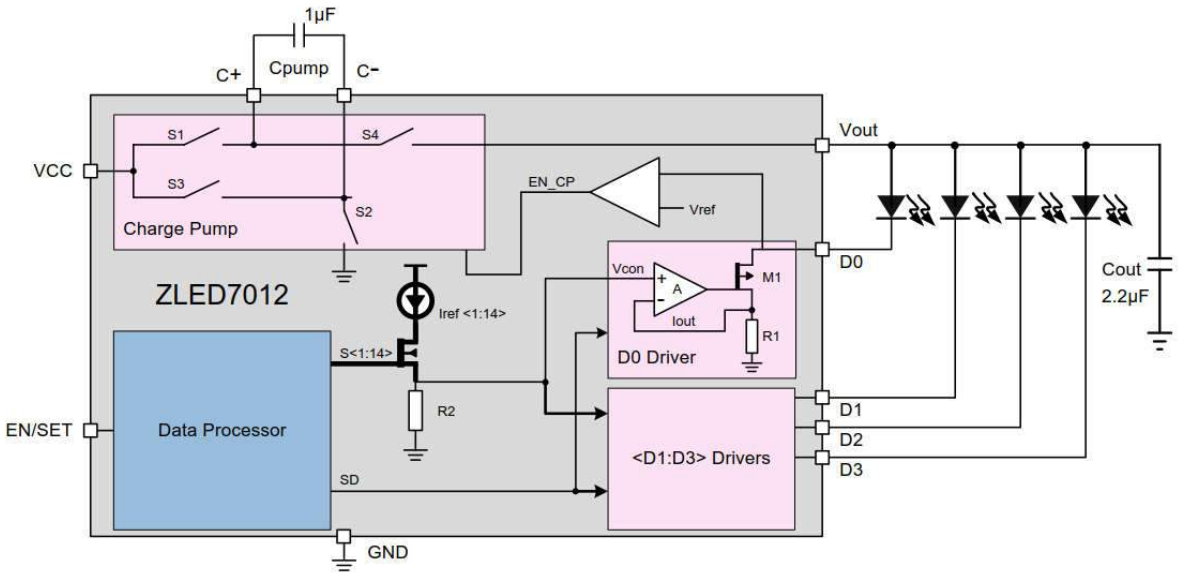

Figure S5. Block diagram of ZLED7012.

Figure S6

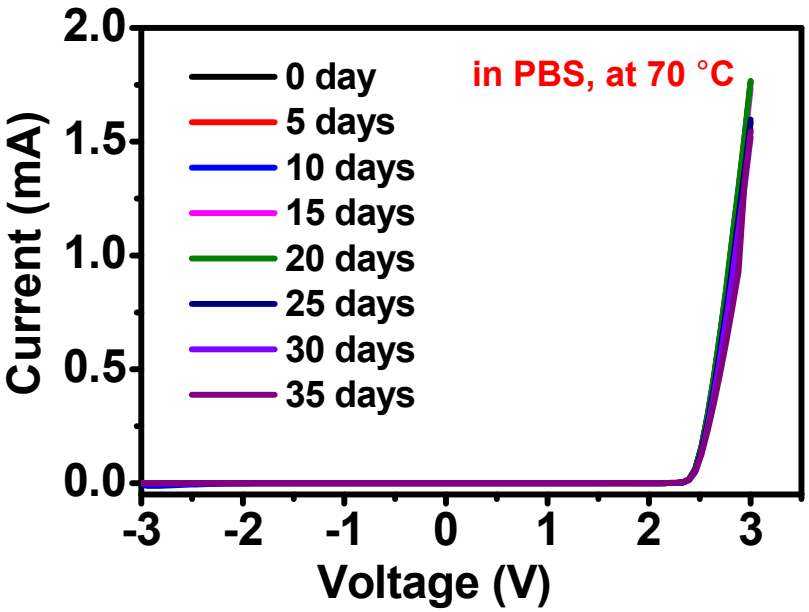

Figure S6. Representative current-voltage characteristics of a micro-LED probe soaked in phosphate buffered saline (PBS) solutions at 70 °C.

Figure S7

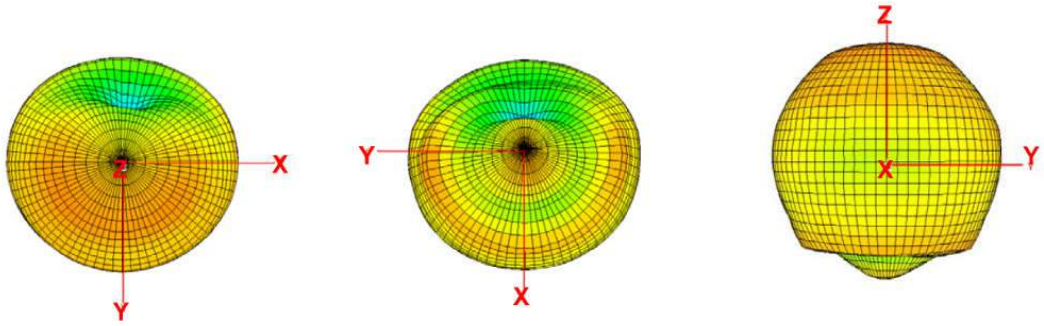

Figure S7. 3D gain pattern of the ceramic chip antenna H2U34WGTQW0100 (extracted from its manual).

Figure S8

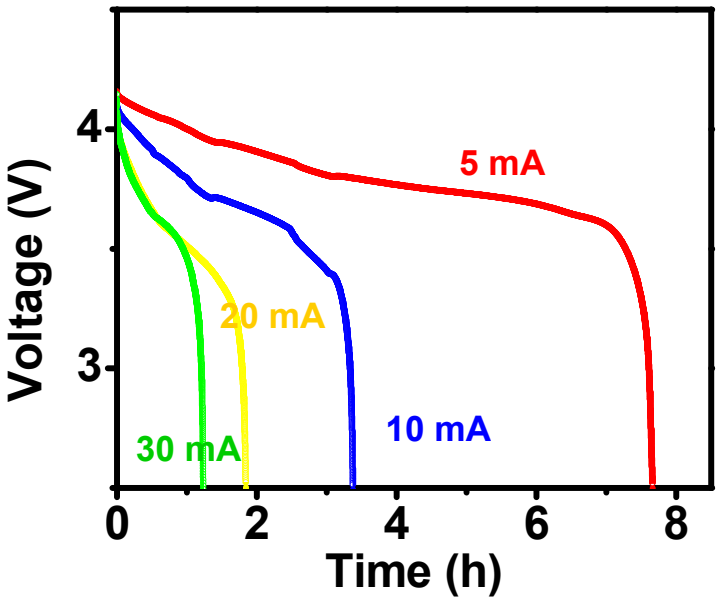

Figure S8. Discharge curves of the lithium ion battery at currents of 5 mA, 10 mA, 20 mA and 30 mA (Model 041015, capacity 35 mAh).

Movie S1

Movie S1. Independent control of multiple micro-LED probes.

Link: https://youtu.be/bOR630Dba3g

Movie S2

Movie S2. Optogenetic modulating the locomotion of a mouse by optically stimulating the CnF.

Link: https://youtu.be/xEdxpAcUeZY

Movie S3

Movie S3. Independent control of 2 mice moving in an arena.

Link: https://youtu.be/m7LAUZSZoDA